Title

Experimental study of a plasma-filled backward wave oscillator

Authors
Zhai, X
Garate, E
Prohaska, R
et al.

Publication Date
1992-12-01

EXPERIMENTAL STUDY OF A PLASMA-FILLED BACKWARD WAVE OSCILLATOR

X. Zhai, E. Garate, R. Prohaska, A. Fisher, G. Benford

Physics Department, University of California, Irvine, CA 92717

Abstract

We present experimental studies of a plasma-filled X-band backward wave oscillator (BWO). Depending on the background gas pressure, microwave frequency upshifts of up to 1 GHz appeared along with an enhancement by a factor of 7 in the total microwave power emission. The bandwidth of the microwave emission increased from $\leq$0.5 GHz to 2 GHz when the BWO was working at the RF power enhancement pressure region. The RF power enhancement appeared over a much wider pressure range in a high beam current case (10-100 mT for 3 kA) as compared to a lower beam case (80-115 mT for 1.6 kA). The plasma-filled BWO has higher power output compared to the vacuum BWO over a broader region of magnetic guide field strength. Trivelpiece-Gould modes (T-G modes) are observed with frequencies up to the background plasma frequency in a plasma-filled BWO. Mode competition between the Trivelpiece-Gould modes and the X-band TM_{01} mode prevailed when the background plasma density was below 6×10^{11} cm^{-3}. At a critical background plasma density of $n_{cr} \cong 8 \times 10^{11}$ cm^{-3} power enhancement appeared in both X-band and the T-G modes, with mode collaboration. Power enhancement of the S-band in this mode collaboration region reached up to 8 dB. Electric fields measured by Stark-effect method were as high as 34 kV/cm while BWO power level was 80 MW. These electric fields lasted throughout the high power microwave pulse.

Introduction

Intense relativistic electron beam excitation of slow wave structures has been an active subject since the possibility was first confirmed by Nation[1] in 1972. Many vacuum slow wave devices have been studied [2-6] since, with conversion efficiency of beam kinetic energy into microwaves as high as 30%. Using current pulse power technology, vacuum backward wave oscillators (BWOs) can emit microwave power as high as 1 GW[7-9]. Injecting plasma into the slow wave structure[10,11] enhances power emission by factors of 3 to 8. Introducing plasma into the BWO increased power output and efficiency. However, some of the basic mechanisms of the system are still not well understood. All previous plasma-filled BWO experiments concentrated on producing higher power microwaves, higher efficiency and longer pulse. The goals of this work were to study the effect background plasma had on the microwave frequency and bandwidth of the output radiation in a high power plasma filled BWO; to study the plasma modes (Trivelpiece-Gould modes) in the plasma-filled BWO and their effect on the BWO waveguide mode (TM_{01}); and to measure the electric field in the plasma-filled BWO using light emission from the background plasma via the Stark shift.

Experimental Setup

In our experiment (Fig. 1), a Marx capacitor bank generates a 650 kV, 2 kA voltage pulse with 500 ns pulse duration. The electron beam was produced by field emission from a graphite cathode. The beam is annular with 1.8 cm diameter and 2 mm thickness, and is injected into the BWO along a guiding magnetic field of 6-16 kG. Our plasma was produced by background helium ionization by the beam. The BWO is a cylindrical waveguide with a periodically varying wall radius, R(z), sinusoidally rippled about the mean radius, R_0, such that $R(z)=R_0+h\cos(k_0 z)$, $k_0=2p/z_0$, where h=0.45 cm is the ripple amplitude, z_0=1.67 cm is the period and R_0=1.45 cm. An X-band horn placed 2 m away received the RF generated by the BWO. The RF was guided by waveguide to a screen room, where the RF was split and detected by an X-band crystal detector and an X-band 8-channel spectrometer which covered frequencies 8.2<f<12.4 GHz. Each channel covered about 500 MHz. There was an observation window on the 9th ripple of the BWO for the electric field measurement. Two optical lenses collected photons from the center of the BWO then focused the photons onto two optical fibers, which guided the light to two spectrometers in the screen room[12]. One spectrometer "looked" at the helium allowed line λ=501.56 nm and the other one "looked" at the forbidden line λ=663.20nm. Both spectrometers had reciprocal linear dispersion of 0.7nm/mm. The allowed and forbidden photons were then recorded by two fast photomulitipliers. Electric fields in the system can be calculated by the ratio of the allowed line and the forbidden line intensity[13]. The observation window on the BWO was also used for the T-G modes measurement. A coaxial cable extended through one window into the BWO with the center conductor acting as a microwave antenna. Microwaves went through more than 30 meters of RG-9 cable, then were measured by a crystal detector, or by an 8 channel S-band (2.6 GHz<f<3.9 GHz) and J-band (5.85 GHz<f<8.2 GHz) microwave spectrometer. Each channel of the S-band spectrometer covered approximately 160 MHz bandwidth with the J-band channels covering approximately 294 MHz bandwidth. We measured frequencies between 3.9 GHz and 5.85 GHz with high pass filters, since a C-band spectrometer was not available to us. Frequency resolved measurements below 2.6 GHz were not made due to a lack of diagnostic equipment. In the X, J and S-band spectrometers the filters had 50 dB stopband insertion loss with 0.9 dB passband insertion loss. The plasma density was measured by a heterodyne microwave interferometer. In order to avoid strong X-band TM_{01} radiation and to not modify the oscillator, we replaced our BWO with a stainless steel tube of 10 mm radius, keeping anode and cathode geometry the same. Since the X-band radiation consistently arrived 140 ns ($\pm$10 ns) into the beam pulse, we could correlate the microwave signal with the plasma density measurement at the turn on of the

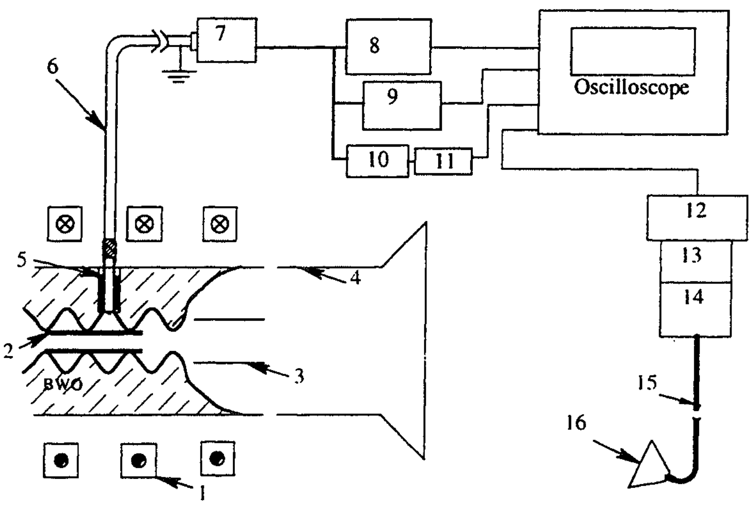

1. B field coils
2. Electron beam
3. Beam dump
4. Drift chamber
5. Antenna
6. 30 m RG-9 cable
7. S-band waveguide
8. S-band rf spectrometer
9. J-band rf spectrometer
10.High pass filter
11. Detector
12. X-band detector
13. X-band bandpass filter
14. Attenator
15. 20 m X-band waveguide
16. X-band recivibg horn

Fig. 1 Experimental setup

microwaves, this method likely underestimates the plasma density during the RF pulse, because of plasma production in the background helium due to the high RF field.

Experimental Results

Our vacuum BWO efficiency of converting beam kinetic energy into RF radiation was about 5%. Depending on the beam current, the RF power output was between 30 MW to 100 MW in vacuum with a frequency of 8.3 GHz. The RF pulse duration was 50~150 ns depending on the RF power output level, As the RF power output increased the RF pulse duration decreased. As we added helium to the BWO, we observed a power increase, frequency upshift and bandwidth increase in the RF output. At low gas pressure (under 10 mT) and beam current of 3 kA only channel 1 (center frequency, f_c=8.46 GHz) and 2 (f_c=8.99 GHz) of the X-band spectrometer detected microwave signal and the signal in channel 1 was 1.5 ~2 times larger. However, in the pressure region where the enhancement in RF power was observed (between 50 mT to 80 mT), signals appeared in the first four channels of the spectrometer and channel 3 gave the maximum output. This indicted a frequency upshift of 1 GHz. Fig. 2(b) shows a shot taken at 60 mT with 3 kA beam current. If we sum the signal output from all channels of the spectrometer in Fig. 2(b) and compare to the signal in Fig. 2 (a), it is more than 7 times larger. Comparison also indicated the bandwidth of the microwave emission increased from ≤0.5 GHz in vacuum to 2 GHz. We observed similar frequency upshift and bandwidth increase for the 1.6 kA beam case as well. Microwave emission bandwidth as a function of the background helium pressure is shown in Fig. 3. The percentage bandwidth $\Delta f/f_0$ changed from ≤5% in vacuum to 25% at the pressure which gave maximum power enhancement. The RF power output as a function of the background helium

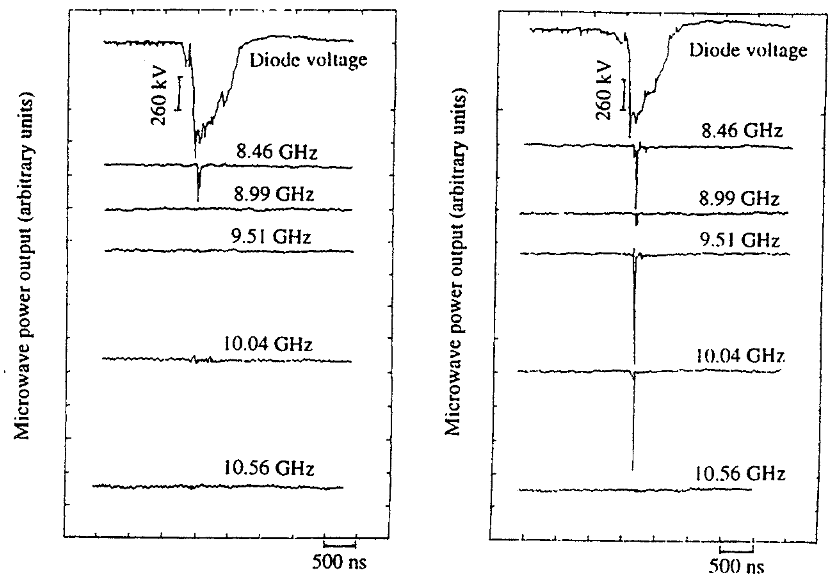

Fig. 2 Beam voltage and RF signal output from the RF spectrometer. (a) vacuum, (b) with plasma

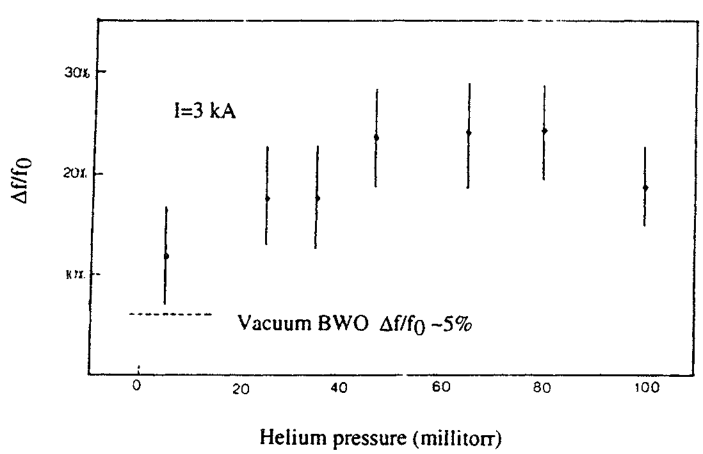

Fig. 3 RF output bandwidth vs background gas pressure

pressure was measured for two different beam currents (1.6 and 3 kA). It is interesting to note that in the 3 kA case,) we observed RF power enhancement over a wider pressure range (10 ~100 mT, while in the 1.6 kA case the RF power enhancement appeared only in a narrow pressure range (80 ~ 100 mT).

Using the antenna placed in the BWO, we detected broadband low frequency microwave radiation up to the plasma frequency of the background plasma. This broadband low frequency emission appeared only with plasma present in the BWO, at frequencies below the cutoff frequency of the plasma-filled BWO and lower than f_p. Power and pulse duration depended on n_p. When the background helium pressure was lower than 70 mT (n_p<4x10^{11} cm^{-3}, f_p<5.7 GHz), no RF signal was detected in the J-band spectrometer. RF signals appeared in every channel of the S-band spectrometer with about the same amplitude and pulse duration. The T-G mode emission (f<5.7 GHz) showed correlation with the X-band TM_{01} mode emission. As in Fig.4 T-G mode power emission always dropped when the TM_{01} mode peaked. This mode competition appeared every shot for about 100 shots when n_p<4x$10^{11}$$cm^{-3}$. As plasma density rose to 4x10^{11} cm^{-3} the TM_{01} mode power output showed no change. However, the T-G mode emission power gradually increased by a factor of 2 over a plasma density change of 2 to 4x10^{11} cm^{-3} (4 GHz <f_p<5.7 GHz). As the pressure reached 100 mT (n_p~7x10^{11} cm^{-3}, f_p=7.5 GHz), RF signals appeared in the first 7 channels (8th channel overlapped with the X-band TM_{01} emission) of the J-band spectrometer and every channel of the S-band spectrometer. The S and J-band spectrometer signals had a pulse duration of ~100 ns. RF signals in J-band had smaller amplitude compared with that of the S-band. However, the coupling efficiency of the antenna as a function of the frequency and the presence of the S-band waveguide (Fig. 1) prevent determination of a quantitative difference in S and J-band signals.

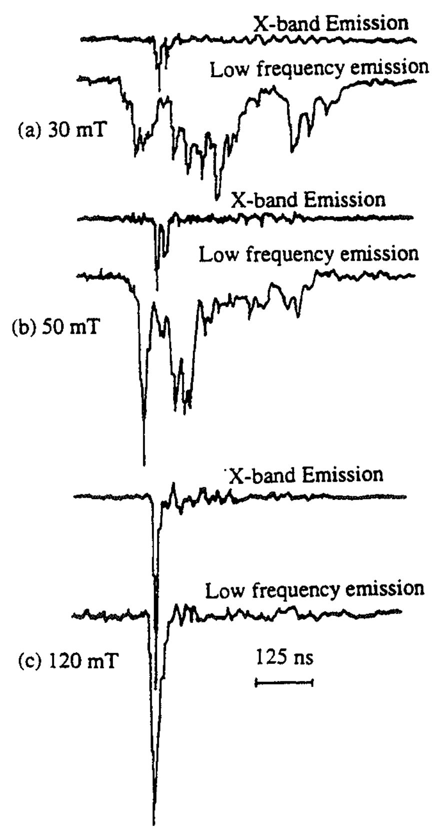

Fig. 4 Oscilloscope traces of the X-band (8.2-10.2 GHz, measured by X-band crystal detector) and the T-G modes (measured by a crystal detector) microwave signals (2 GHz<f<5.7 GHz).

As the background helium pressure reached 120 mT (n_p=n_{cr}~8x10^{11} cm^{-3}) a simultaneous peak in the TM_{01} mode and the T-G modes (both S and J-band) was observed. A sudden enhancement appeared in the S-band T-G mode peak power of up to 8 dB. The J-band RF signal amplitude increased with the S-band RF but no more than 3 dB. The X-band TM_{01} mode emission increased for 6x10^{11} cm^{-3}<n_p<8x10^{11} cm^{-3} and peaked at n_{cr}. Power enhancement was typically a factor of 3 at n_{cr}, but up to a factor of 6 in some shots. Given the error in the plasma density measurement, the background plasma density could be as high as n_p~9.5x10^{11} cm^{-3} (f_p~8.8 GHz) when the TM_{01} mode and T-G modes power emission are enhanced. This could indicate the possibility that part of the enhanced X-band signal was a result of T-G mode radiation. Although the absolute T-G modes power emission was not calibrated, we found that the power carried by the T-G modes emission (in J-band) was at least 27 dB less than the X-band TM_{01} mode. For plasma density $n_p > 8 \times 10^{11}$ cm^{-3}, power emission in the TM_{01} mode gradually decreased, and the T-G modes pulse became much shorter (~50 ns) but their amplitude kept increasing (both S and J-band). When the pressure reached 170 mT the J and S-band power emission was 2-3 times larger than that for 120 mT.

Using a spectroscopic method to measure the electric field distribution in a relatively high noise level system is very efficient and convenient. We choose the four energy-level system (3^1P, 3^1D, 2^1P, 2^1S) of helium I for the spectroscopic measurement. Transitions from 3^1P to 2^1S (λ_A=501.56 nm) and from 3^1D to 2^1P (λ=667.80 nm) are allowed, and the transition from 3^1P to 2^1P is forbidden (l_F=663.20 nm) in the electric dipole approximation. In a perturbing electric field, energy levels 3^1D and 2^1P are mixed, under this condition, it is possible to see photons from the forbidden line. The perturbing electric field strength can be calculated by the forbidden (λ_F=663.20 nm) and allowed (λ_A=501.56 nm) line intensity ratio I_F/I_A,,(Ref. 13):

$$E = 305.8\left(\frac{I_F}{I_A}\right)^{0.54} \mathrm{kV/cm}, \qquad (1)$$

We increased the diode A-K gap reducing the beam current to ~1 kA to get a longer microwave pulse. We counted photon numbers in each time interval for both the forbidden and allowed lines in each shot, then averaged over ~100 shots. The ratio of the average photon numbers in the forbidden and allowed lines was used to calculate the electric field using equation (1).

Fig. 5 shows the results of the electric field measurement in the plasma-filled BWO when the RF was enhanced by the background plasma by a factor of 2 over its vacuum counterpart. The measured RF power was 80 MW$\pm$10 MW and the RF pulse duration (FWHM) was ~60 ns. Fig. 5 shows the electric fields lasted only as long as the microwave pulse, peaking at 34 kV/cm, then dropped to ~12 kV/cm. To estimate how much microwave power this field strength implies, assume a smooth wall tube with radius of the average radius of the BWO, R_0=1.9 cm. Assuming a TM_{01} mode propagating along the axis, and the average electric field of the RF equal to our measured value $\overline{E} = \sqrt{<E^2>}$ =34 kV/cm, then we get a power of S=17$\pm$10 MW, with the uncertainty due to the error in electric field measurement (photon number fluctuation from shot to shot). This 34 kV/cm electric field is lower than we expected from the direct RF power measurement, since it gives a power flux lower than the measured X-band power of 80 MW$\pm$10 MW. The electric field of the electron beam charge is not important here, since the plasma density was 8×10^{11} cm^{-3} and the beam density was 5×10^{11} cm^{-3}, so the beam was charge neutralized. However, this calculation assumes a smooth tube with a TM_{01} mode propagating axially with average electric field

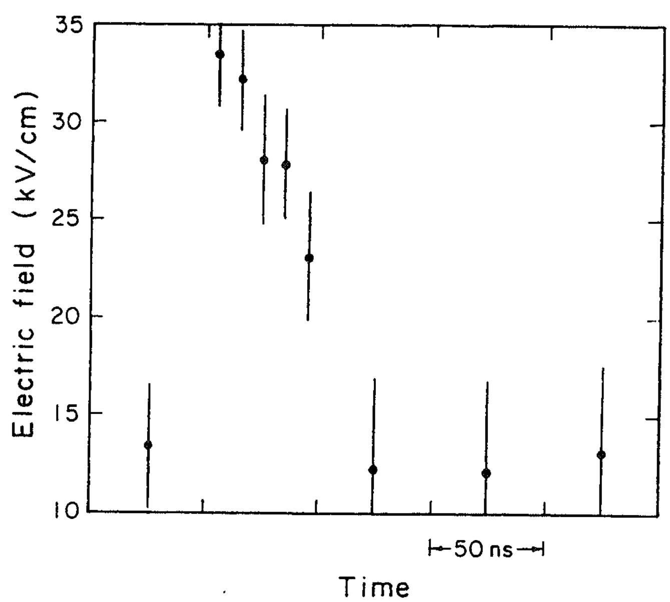

Fig. 5 Electric field vs time when the BWO RF power was enhanced by the background plasma.

the same as our measured fields. The real situation differs greatly from this, since the BWO RF electric field is strong near the wall. Our optical system focused in the BWO center when we measure E. Since we collect most of our photons from the center of the BWO our measured E field is much lower than the peak electric field. This may explain why the estimated microwave power is much lower than the measured RF power. To do an accurate power calculation requires knowing $\vec{E}(\vec{r})$ in the plasma filled BWO, a very complex calculation. (see Ref. 14)

In conclusion, we measured the average electric field strength as a function of time on our BWO axis, where the relativistic electron beam, high power microwaves and plasma interact. While the microwave power output was enhanced by the background plasma, the electric field peaked at 34 kV/cm and lasted only as long as the high power RF pulse (~80 MW), about 50 ns. We measured the T-G modes with frequencies up to the background plasma frequency in our plasma-filled BWO. This could be the "dense spectrum" of plasma waves as discussed in Ref. 15. At a critical plasma density the T-G modes and the BWO TM_{01} mode output power were simultaneously enhanced. The T-G mode measurement and the electric field measurement, to the best of our knowledge, have not been done previously for a device of the kind.

We thank Dr. K. Kato, David Sar and General Dynamics, Pomona Division, for the use of their equipment. This work was supported by AFOSR under contract # 90-0255.

References

1. J. A. Nation, Appl. Phys. Lett 17, 491 (1970).
2. Y. Carmel, J. Ivers, R. E. Kriel, and J. Nation, phys. Rev. Lett. 33, 1278 (1974)
3. M. Friedman, Appl. Phys. Lett 26,376 (1975).
4. V. I. Belousov, V. V. Bunkin, A. V. Gaponov-Grekhov, et al., Sov. Tech. Phys. Lett. 4, 584 (1978).
5. V. S. Ivanov, N. F. Kovalev, S. I. Krementsov, and M. D. Raizer, Sov. Tech. phys. Lett. 4,329 (1978).
6. Yu. V. Tkach, Ya. B. Fainberg, N. P.Gadetskii, et al., Ukr. Fiz. Zh. 23, 1902 (1978).
7. V. S. Ivanov, S. I. Krementsov, V. A. Kutsenko, M. D. Raizer, and A. A. Ruchadze, Proceedings of the International Topical Conference on High Power Electron and Ion Beams, Vol. II, Novosibirsk 679 (1979).
8. Yu. F. Bondar', S. I. Zavorotnyi, A. L. Ipatov, N. I. Karbushev, N. F. Kovalev, O. T. Loza, G. P. Mkheidze, and L. E' Tsopp, Sov. J. Plasma Phys. 9(2) 223, (1983).
9. V. S. Ivanov, S. I. Krementsov, V. A. Kutsenko, M. D. Raizer, A. A. Rukhadze, and A. V. Fedotov, Sov. Phys. Tech. Phys. 26 (5),580 (1980).
10. A. A. Kolomenskii, E. G. Krastelev, G. O. Meskhi, and B. N. yablokov. Second Symoposium on Collective Acceleration Methods, Dubna, 160, (1976) [in Russian].
11. Y. Carmel, K. Minami, R. A. Kehs, W. W. Destler, V. L. Granatstein, D. Abe, and W. L. Lou, Phys. Rev. Lett. 62,(20) 2389 (1989).
12. A. Dovrat and G. Benford, Phys. Fluids B1 (12), 2488 (1989).
13. K. Kawasaki, T. Usui and T. Oda, J. phys. Soc. Jpn. 51, 3666 (1982)
14. Minami, Y. Carmel, V. L. Granatstein, W. W. Destler, W. R. Lou, D. K. Abe, R. A. Kehs, M. M. Ali, T. Hosokawa, K, Ogura and T. Watanabe, IEEE Transations on Plasma Science. 18, 537 (1990).
15. W. R. Lou, Y. Carmel, W. W. Destler, and V. L. Granatstein, Phys. Rev. Lett. Oct, 28 (1991).